Sensors and Actuators B 263 (2018) 377–386

Contents lists available at ScienceDirect

Sensors and Actuators B: Chemical

journal homepage: www.elsevier.com/locate/snb

Development of a third generation biosensor to determine hydrogen peroxide based on a composite of soybean peroxidase/chemically reduced graphene oxide deposited on glassy carbon electrodes

César Horacio Díaz Nieto[a], Adrian Marcelo Granero[a], Jimena Claudia Lopez[a], Gastón Dario Pierini[a], Gustavo Javier Levin[b], Héctor Fernández[a,*], María Alicia Zon[a,*]

[a] Departamento de Química, Facultad de Ciencias Exactas, Físico-Químicas y Naturales, Universidad Nacional de Río Cuarto, Agencia Postal No. 3, (5800) Río Cuarto, Argentina

[b] Centro de Investigaciones y Transferencia de Entre Ríos (CITER)-CONICET-UNER, Presidente Perón 64, (2820) Gualeguaychú, Entre Ríos, Argentina

ARTICLE INFO

Article history:
Received 15 August 2017
Received in revised form 22 January 2018
Accepted 11 February 2018
Available online 13 February 2018

Keywords:
Biosensor
Soybean peroxidase enzyme
Chemically reduced graphene oxide
Hydrogen peroxide
Compound II

ABSTRACT

A third generation enzymatic biosensor is developed to determine H_2O_2. The biosensor is based on the use of a composite obtained from soybean peroxidase enzyme and chemically reduced graphene oxide deposited at glassy carbon electrodes. Experiments were carried out in 0.1 M phosphate buffer solutions, pH 7.0.Cyclic voltammograms of the biosensor show two reduction peaks centered at about 0.15 and −0.4 V, respectively. A quasi-reversible redox couple is defined in the region of potentials of the first peak, which is assigned to the reduction/oxidation of compound II involved in the catalytic cycle of peroxidases. The surface concentration of the electroactive enzyme was $(1.1 \pm 0.2) \times 10^{-10}$ mol cm^{-2}. Values of 0.33 and 0.04 s^{-1} were determined for the cathodic charge transfer coefficient and the heterogeneous electron transfer rate constant, respectively. UV–vis spectroscopy and scanning electron microscopy (SEM) were used to demonstrate the chemical reduction of graphene oxide. Electrochemical impedance spectroscopy was used to characterize the different stages in the process of the electrode surface modification.

Amperometric measurements were performed at a potential of −0.090 V vs. Ag/AgCl. Current responses were linear in the concentration range from 1.5×10^{-7} to 3.0×10^{-6} M. The limit of detection, limit of quantification, reproducibility, and repeatability were 5×10^{-8} M, 1.5×10^{-7} M, 9%, and 4%, respectively. The biosensor was stable during five days. The Michaelis Menten apparent constant was 1.6×10^{-6} M. The presence of uric acid, glucose, dopamine and ascorbic acid do not interfere in the determination of H_2O_2.

The biosensor was applied to the determination of H_2O_2 in commercial contact lens care solutions. Good accuracy and recovery parameters were obtained.

1. Introduction

The H_2O_2 is produced during the oxidation of different biological substrates by dissolved oxygen in the presence of the corresponding oxidase enzyme, i.e., glucose [1]. H_2O_2 is widely used as an oxidizer, disinfectant, and bleaching agent in various industrial and household products [1,2]. The H_2O_2 is hazardous because of its rapid conversion to the hydroxyl radical, either by exposure to ultraviolet light [3] or by interaction with transition metals [1,3]. The determination of H_2O_2 is important for different causes, such as quantifying its concentration as an effective agent in solutions that ensure disinfection, to verify its elimination after the disinfection of pipes, surfaces, soft drink and juice industries, etc. and to control its use as an additive not allowed. Therefore, different techniques have been used for the determination of H_2O_2 such as fluorometry, volumetry, chemiluminescence, spectrophotometry and electrochemistry [4]. Electrochemical techniques are preferred because of their low cost, fast response time and high sensitivity [5]. Pt electrodes allow the direct determination of H_2O_2 due to its catalytic activity [6]. However, the use of enzymatic electrodes based on the direct electron transfer between an immobilized enzyme and the electrode surface is an interesting proposal due to its simplicity and high sensitivity [7]. One of the most widely used enzymes in the development of biosensors for the determination of H_2O_2 is the horseradish peroxidase (HRP) due to its high stability and catalytic activity [6,8–12].

* Corresponding authors.
E-mail addresses: cdiaznieto@cidmeju.unju.edu.ar (C.H. Díaz Nieto), agranero@exa.unrc.edu.ar (A.M. Granero), jlopez@exa.unrc.edu.ar (J.C. Lopez), gpierini@exa.unrc.edu.ar (G.D. Pierini), glevin@conicet.gov.ar (G.J. Levin), hfernandez@exa.unrc.edu.ar (H. Fernández), azon@exa.unrc.edu.ar (M.A. Zon).

https://doi.org/10.1016/j.snb.2018.02.094
0925-4005/

The soybean peroxidase enzyme (SPE) is also part of the large family of plant peroxidases (class III). Its structure is similar to HRP, has the same prosthetic group and catalytic mechanism [13]. It is known since the nineties [14], and has not been as well studied as the HRP [9]. SPE has better properties than HRP such as is less susceptible to heme group loss, and H_2O_2 inactivation [14,15], and can maintain its bioactivity over a wide pH range (from 3 to 10).SPE has a thermal stabilityhigherthan HRP, i.e., SPE is stable up to 86 °C compared to 74 °C of HPR [9,16]. SPE has also a conformational stability higher than HRP under physiological conditions, i.e., 43.3 vs.17 kJ mol^{-1} [9]. Thus, all these characteristics make SPE a good biological element for the development of biosensors. Its catalytic cycle both in solution and on the electrode surface is well known [17]:

Thus, in the first stage of the catalytic cycle,the active site of the enzyme reacts with H_2O_2 with a rate constant k_1. The enzyme oxidizes, losing two electrons, giving the compound I (Cp I), which contains a central oxyferril (Fe^{+4}) group and an organic radical cation, $R^{+\bullet}$. The Cp I is then reduced by one electron for giving the compound II (Cp II), which is then reduced by another electron to regenerate the enzyme in its native state. $k_{ET,1}$ is the electron transfer rate constant of the Cp I/Cp II redox couple and $k_{ET,2}$is that of the Cp II/SPE redox couple [17].

The direct electron transfer occurs between the active site of the enzyme and the electrode surface in the third generation biosensors, without the participation of redox mediators [18]. However, the direct electron transfer is very difficult with conventional electrodes because the active site of several enzymes is located in a hydrophobic cavity of the enzyme.The probability of direct electron transfer decreases exponentially as the distance between the active site of the enzyme and the electrode surface increases [19]. This disadvantage can be solved if a suitable material is chosen to modify the surface of the electrode.

It is well known that graphene is a very suitable material for electrochemical applications due to its large surface area and high electrical conductivity [20]. It favors a high heterogeneous electron transfer rate due to the large number of edges per mass of material involved [21]. Graphene oxide (GO) has a wide variety of oxygen-containing reactive groups such as carboxyl's, carbonyls, epoxies', and hydroxyls attached to a network of C sp^3 structure.Reduced graphene oxide (RGO) is the main graphene material used in electrochemical applications, mainly in the development of sensors and/or biosensors [22]. RGO has a sp^2 carbon content higher than GO. However,it maintains oxygen groups in its basal plane. Chemically reduced graphene oxide (CRGO) has a similar structure but not equal to graphene, having a very defective structure compared to graphene [23].

In this paper, we propose a third generation biosensor to determine H_2O_2. It is based on the use of a composite obtained from SPE and CRGO deposited on glassy carbon electrodes. Experiments were carried out in 0.1 M phosphate buffer solutions (PBS), pH 7.0. The kinetic parameters of the direct electron transfer between the SPE and the electrode surface such as the cathodic charge transfer coefficient and the heterogeneous electron transfer rate constant were determined by cyclic voltammetry (CV), and electrochemical impedance spectroscopy (EIS). UV–vis spectroscopy and scanning electron microscopy (SEM) were used to demonstrate the chemical reduction of GO. EIS was used to characterize the various stages of electrode surface modification. Amperometric measurements were used to determine the Michaelis Menten apparent constant, and different analytical parameters such as linear concentration range, limit of detection (LOD), limit of quantification (LOQ), reproducibility, repeatability and stability of the biosensor. The amperometric measurements were also used to demonstrate that uric acid, glucose, dopamine and ascorbic acid do not interfere in the determination of H_2O_2. The biosensor was applied to the determination of H_2O_2 in commercial contact lens care solutions using the standard addition method. Good accuracy and recovery parameters were obtained.

2. Materials and methods

2.1. Purification of soybean peroxidase enzyme

SPE was purified from soybean hulls as a single isoenzyme. Therefore, soybean hulls were soaked overnight with distilled water at 4 °C. After that, suspension was clarified by centrifugation at 10000 rpm during 15 min and the supernatant was concentrated by ultra-filtration with a hollow-fiber cartridge of MWCO 10 kDa (Fresenius Polysulfone®). Supernatant was loaded to a pre-packed Q FF column (GE Healthcare, Piscataway, USA) previously equilibrated with a buffer solution (25 mM sodium phosphate buffer, pH 6.0). Protein elution was performed with a 20 min-gradient of NaCl from 0 to 1 M in the same buffer solution, at a flow rate of 1.0 mL/min. Elution fractions were recovered and absorbance at multiple wavelengths (280, 215 and 403 nm) and peroxidase activity were measured. Fractions containing peroxidase were pooled and ammoniun sulfate was added up to 0.75 M. Suspension was loaded to a pre-packed Phenyl HP column (GE Healthcare, Piscataway, USA) equilibrated with 50 mM sodium phosphate buffer, pH 6.0, and 0.8 M ammonium sulfate. The elution was performed with distilled water, at a flow rate of 1.0 mL/min, and the effluent was monitored measuring the absorbance at 280, 215 and 403 nm, and the peroxidase activity was determined. All chromatographic runs were carried out with ÄKTA Purifier equipment (GE Healthcare, Piscataway, USA).

Reaction mixture to determine the enzymatic activitywas composed by 20 μM guaiacol and 8 mM H_2O_2 in 1 mL of 100 mM PBS, pH 5.5, at 25 °C. After addition of a 50 μL sample, absorbance at 470 nm was recorded within 90 s. Activity calculations were performed as described by Tjissen [24].

2.2. Other reagents

0.1 M PBS were prepared by mixing equal concentrations of K_2HPO_4 and KH_2PO_4 (Merck p.a.). The pH was adjusted by adding 0.1 M NaOH or 0.1 M HCl as appropriate, both Merck p.a. Hydrazine sulfate was purchased from Sigma-Aldrich.

The enzyme concentration was determined through measurements of UV–vis absorption at $\lambda = 403$ nm ($\varepsilon_{Enz}^{403} = 0.9 \times 10^{-5}\ M^{-1}\ cm^{-1}$) [8,9].

H_2O_2 (Merck p.a.) solutions were prepared daily. Their concentrations were determined through measures of uv–vis absorption at $\lambda = 240$ nm ($\varepsilon_{H_2O_2}^{240} = 43.6\ M^{-1}\ cm^{-1}$) [25].

The contact lens care solution was purchased in a local Optic store. The concentration of H_2O_2 indicated on the label was 3% (w/v). A 1:50 dilution of the commercial sample was performed in water and the absorbance at 240 nm was 0.785. Therefore, the concentration of H_2O_2 in the commercial sample obtained by UV–vis spectroscopy was 3.08% in very good agreement with that declared by the manufacturer.

All solutions were prepared with bi-distilled water, which was distilled in the presence of a basic solution of $KMnO_4$.

2.3. Apparatus

CV and amperometric measurements were performed using a BAS Epsilon potentiostat, with electrochemical software incorporated. In CV, the scan rate, v, was varied from 0.010 to 0.200 V s^{-1}. EIS measurements were performed using an AutoLab PGSTAT 30 potentiostat, Eco-Chemie, Utrecht, The Netherlands, with the FRA

4.9 software incorporated. Some EIS measurements were performed in the presence of 5×10^{-3} M $[Fe(CN)_6]^{-4/-3}$ + 0.1 M KCl aqueous solutions. The applied potential was 0.23 V, which corresponds to the formal potential of the redox couple. Other EIS measurements were carried out in 0.1 M PBS, pH 7.0 at a potential of 0.26 V, which corresponds to the formal potential of Cp II/SPE redox couple. The amplitude of the sinusoidal perturbation was 5 mV. The AC frequency was varied from 0.1 Hz to 10 kHz. The impedance spectra were fitted using the EIS Spectrum Analyser 1.0 [26].

A conventional three electrode cell was used in all electrochemical measurements. The working electrode was a glassy carbon (GC) disk (BAS, dia. = 3 mm). Ag/AgCl (3 M NaCl) and a large area Pt sheet were used as the reference and the counter electrodes, respectively.

The solutions were deoxygenated by bubbling pure argon for 15 min prior to measurements.

An UV–vis spectrophotometer, Hewlett Packard, Model HP8453 was used for spectrophotometric measurements. The cells had an optical path of 1 cm.

SEM images were obtained with a Field Emission Gun Scanning Electron Microscopy (FE-SEM, Zeiss, ΣIGMA model).

2.4. Synthesis of CRGO

GO was synthesized following the methodology proposed by Marcano et al. [27]. CRGO was synthesized following the methodology proposed by Guo et al. [28]. Therefore, 5 mL of theGO homogeneous dispersion (0.5 mg mL^{-1}) were mixed with 375 μL ammonia solution (28%) and, then 10 μL of hydrazine sulfate (50% w/w) was added and was carried out to a final volume of 10 mL with bi-distilled water. After vigorously stirring during a few minutes, the mixture was heated to a 60 °C in a water bath during 3.5 h. The mixture was then cooled to room temperature; the dispersion was centrifuged and washed three times with water to remove excesses of hydrazine. Finally, water was added to a volume of 1.5 mL to obtain a CRGO dispersion of about 1.7 mg mL^{-1}. This solution was sonicated prior to its use.

A first characterization of synthesized CRGO was performed by visual inspection. Thus, while the GO dispersion is brown, that of CRGO is black. On the other hand, the UV–vis spectrum of CRGO showed a marked increase in absorbance at λ about 230 nm, which is assigned to π–π* transitions of the aromatic double bonds; and a decrease of the shoulder at about λ = 290 nm, which is assigned to n-π* transitions of C=O groups, when it is compared with the GO UV–vis spectrum (Fig. S1, Supporting Information).

The morphology and structure of GO and CRGO were investigated through SEM images (Fig. S2, Supporting Information). Fig. S2 (A and B) reveals a wrinkled and wavy structure for GO. As shown in Fig. S2 (C and D), two-dimensional material can be observed for CRGO. This structure has more structured layers, irregular, folding and tangled together. The SEM images show particles of various sizes for the CRGO, where the thickness varies between 20 nm and 100 nm. Therefore, exfoliation and morphological changes from GO to CRGO are confirmed from these SEM results. In addition, a visual inspection of SEM images shows that the CRGO has a greater number of parallel ridges and grooves than GO, which gives it a greater rigidity and strength. This can be explained considering the decrease of oxygen-containing groups during the reduction process.

2.5. Preparation of GC/SPE/CRGO composite electrodes

80 μL SPE (28.5 μM) were mixed with 20 μL of the CRGO dispersion (see below). The mixture was sonicated in an ultra sound bath during 7 min and then in a vortex during 30 min. It was then allowed to stand during 12 h at 4 °C. The composite was stable for three months.

5 μL of the SPE/CRGO mixture were deposited on the surface of the GC electrode. The modified electrode was dried at 35 °C. The electrode was washed with water to remove the free enzyme. It was stored at 4 °C when it was not in use. The immobilization of SPE on CRGO occurs by physical adsorption. Similar interactions would occur between the composite and the GC electrode surface. Prior to the modification process, the GC electrode was polished on a wet cloth with alumina of 1, 0.3 and 0.05 μm. The electrode was then rinsed with water, and sonicated in an ultrasonic bath during 3 min. Finally, it was rinsed again with water and dried under argon atmosphere.

2.6. Experimental designs

The construction of the amperometric biosensor to determine H_2O_2 depends on several factors. They are the amount of enzyme and CRGO to be mixed, the pH of the buffer solution, the potential (E) at which the amperometric measurements are performed, the drying temperature of the mixture (T_{drying}) and the amount of mixture deposited on the electrode surface. Thus, a fractional factorial design, 2^{5-1}, was used to study the five factors mentioned above [29].

- **Mixture (x)**: It was varied between 40 and 90%, where x is the amount of enzyme expressed in μL present per 100 μL of the SPE/CRGO mixture (% v/v).
- **pH**: It was varied from 5 to 7.
- **E**: It was varied from −0.4 to 0.3 V vs. Ag/AgCl.
- **T_{drying}**: It was varied in the 25–35 °C range.
- **Amount of mixture SPE/CRGO deposited on the surface of the electrode**: It was varied from 5 to 10 μL.

A composite central design was also used to optimize the significant factorsobtained from fractional factorial design.

3. Results and discussion

3.1. Optimization of the amount of SPE and CRGO in the composite electrode

From the results obtained from the fractional factorial design, it was possible to infer that only two factors are significant: the potential at which amperometric measurements are performed and the amount of enzyme in the SPE/CRGO composite. Thus, the pH was set at 7.0 because the physiological solutions have a pH close to this value.The amount of mixture SPE/CRGO and T_{drying} were set at 5 μL and 35 °C, respectively, considering that the enzyme can maintain its catalytic activity at high temperatures. An advantage of using a T_{drying} = 35 °C is the decrease in the drying time. On the other hand, experiments carried out at T_{drying} higher than 35 °C generated very heterogeneous modified surfaces, containing cracks and lumps.

The two significant factors were then optimized using a composite central design. The levels of the two factors were varied between 40% < x < 93% and −0.4 V < E < 0.30 V (Table S1, Supporting Information). In addition, the selected alpha value was 1.41 to obtain a rotatable design that allows constant prediction variances to be obtained at all points that are equidistant from the design center [30]. The variable to be optimized is the slope of the calibration curve, ΔI_{ss} vs $c_{H_2O_2}$ (see below). The goal of optimization is to obtain the highest value for the slope of the calibration curve.

Fig. S3 (Supporting Information) shows the response surface obtained from the composite central design. From these results, it is possible to infer that there are no interactions between the two factors, so each factor was studied independently. The slope of the calibration curve increased linearly as the potential became

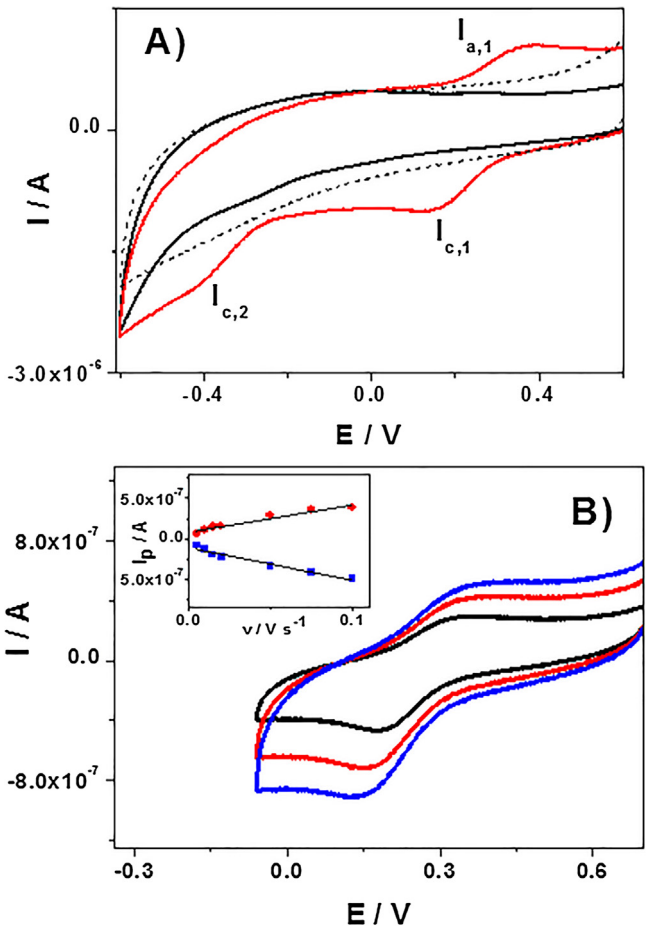

Fig. 1. Cyclic voltammograms recorded in pH 7.0 0.1 M PBS at GC/SPE (-), GC/CRGO (black solid line) and GC/SPE/CRGO (red solid line) electrodes. (B) Cyclic voltammograms recorded at GC/SPE/CRGO electrode in the potential range from 0.7 to −0.1 V at different v; v = 0.050 (black line), 0.075 (red line) and 0.100 V s^{-1} (blue line). The insert of Fig. 2B shows the dependence of I_p with v for both cathodic and anodic peaks. (For interpretation of the references to colour in this figure legend, the reader is referred to the web version of this article.)

more cathodic. However, at potentials lower than −0.090 V, it was not possible to obtain steady-state currents (I_{ss}) either in the blank solution or during the different aggregates of H_2O_2, making it difficult to analyze the data .I_{ss} were achieved in less than 5 min at an E = −0.090 V. Thus, this value was chosen.

On the other hand, as x increased in the composition of the SPE/CRGO mixture the slopes of the calibration curves also increased. The disadvantage is that at values of x greater than 80, amperograms were very noisy and the dispersions were not homogeneous. Thus, the value of x = 80% was chosen.

3.2. Electrochemical behavior of the biosensor

3.2.1. Cyclic voltammetry

Cyclic voltammograms recorded in 0.1 M PBS, pH 7.0at GC/SPE, GC/CRGO and GC/SPE/CRGO electrodes are shown in Fig. 1A.

No voltammetric peak is observed on the GC/SPE electrode, evidencing that the direct electron transfer between the enzyme and the GC electrode surface is not possible. A very small voltammetric peak at approximately − 0.28 V is observed on the GC/CRGO electrode, which would correspond to the reduction of the carboxyl groups present on the surface of the CRGO [31]. Two reduction peaks are observed on the GC/SPE/CRGO electrode, centered at about 0.15 V ($I_{c,1}$) and −0.4 V ($I_{c,2}$). Peak $I_{c,1}$ shows its complementary anodic peak ($I_{a,1}$) when the direction of the potential sweep is reversed (Fig. 1A). These peaks would correspond to the reduction/oxidation of the enzyme immobilized on the modified electrode. Peak $I_{c,2}$ can be assigned to the reduction of ion Fe^{+3} to Fe^{+2} of the heme group of the enzyme. This behavior is in good agreement with others described in the literature. Thus, Gorton et al. [32] determined a formal potential (E_f^o) of −0.3 V for the heme group of peroxidases adsorbed on a gold electrode modified with 4-mercaptoethanol. Brusova and Magner [33] determined an E_f^o = −0.35 V for the same heme group adsorbed on GC electrodes.

The E_f^o of the $Fe^{+3/+2}$ redox couple can vary over a wide range of potentials due to the nature of the sphere of coordination surrounding iron in the heme group and the protein structure that surrounds the heme group [34].

On the other hand, the complementary anodic peak of $I_{c,2}$ is not observed when the direction of the sweep of potential is reversed. This could be because Fe^{+2} interacts with the hydroxyl and/or carbonyl groups present on the electrode surface, inactivating the enzyme, due to the probable formation of compound III [34]. However, when an additional electrochemical reduction of the CRGO present on the electrode surface is carried out by sweeping the potential from −0.5 to −1.7 V, the hydroxyl, and carbonyl groups are reduced. When a new cathodic sweep is performed, from 0.3 to −0.7 V, the complementary anodic peak of $I_{c,2}$ peak is observed (results no shown). However, the corresponding cathodic peak is shifted from −0.4 to −0.22 V. Csöregi et al. [35] found that a sweep to very cathodic potentials causes the denaturation of the enzyme, losing its catalytic activity.

Cyclic voltammograms recorded in the potential range from 0.7 to −0.1 V at different scan rates are shown in Fig. 1B. Li and Dong [36] studied the oxidation/reduction properties of the HRP enzyme on gold electrodes modified with 3-mercaptopropionic acid. These authors found two quasi-reversible oxidation peaks, with E_f^o at 0.175 and 0.5 V, respectively. These peaks were assigned to the HRP/Cp II and Cp II/Cp I redox couples, respectively. Based on these results, we assigned the quasi-reversible redox couple ($I_{c,1}/I_{a,1}$) found for SPE to the formation of compound II. A value of E_f^o = 0.26 V was determined for the Cp II/SPE redox couple, which was estimated as the average of cathodic and anodic peak potentials [37]. The dependence of the peak currents (I_p) of both cathodic and anodic peaks of cyclic voltammograms recorded at GC/SPE/CRGO was linear with v (inset Fig. 1B). This behavior shows that the electrode process is adsorption controlled [37]. The relationship between the anodic and cathodic peak currents was 0.7. The surface concentration of electroactive enzyme was determined using the following equation [37]:

$$\Gamma = \frac{Q}{nFA} \quad (1)$$

Where Γ is the SPE surface concentration, Q is the charge obtained by integrating the voltammetric peaks after subtraction of the blank currents, n is the number of electrons exchanged, F is the Faraday constant and A is the electrode geometric area. A value of $\Gamma = (1.1 \pm 0.2) \times 10^{-10}$ mol cm^{-2} was determined using n = 1. The low percentage of electro-active enzyme on the electrode surface would be explained considering that the enzyme is adsorbed on CRGO surface at random. Therefore, if the enzyme is adsorbed with an orientation where the Fe center is away from the electrode surface, the probability of direct electron transfer is very low. On the other hand, if the enzyme is oriented with the Fe center close to the electrode surface the direct electron transfer is easier, considering that the distance between the electrode surface and the active site of the enzyme is much smaller [38]. The heterogeneous electron

transfer rate constant, k_{ET}, was determined using a methodology proposed by Laviron [39] (Eq. (2)).

$$E_{p,c} = E_f^o + \frac{RT}{\alpha nF}\ln\left(\frac{RTk_{ET,2}}{\alpha nF}\right) - \frac{RT}{\alpha nF}\ln v \quad (2)$$

where $E_{p,c}$ is the cathodic peak potential, α is the cathodic transfer coefficient and R and T have their usual meaning. A plot of $E_{p,c}$ vs. ln v was linear. From the slope and the intercept, values of $\alpha = 0.33$ and $k_{ET,2} = 0.04\,s^{-1}$ were determined. The value of α is in reasonably good agreement with other values obtained for the peroxidase biosensors, i.e., 0.43 for CTS/Hb/3D-Gr/CILE [40]; 0.31 for HRP-Sb-BLM [41]; and 0.39 for HRP/ZrO_2NPs/GCE [42].

3.2.2. Electrochemical impedance spectroscopy

The different stages in the construction of the biosensor were characterized by EIS, which is a powerful technique to study the electrode-solution interface [43].Therefore, these measurements were firstly performed in $[Fe(CN)_6]^{-4/-3}$ + 0.1 M KCl aqueous solutions. The applied potential was 0.23 V, which corresponds to the formal potential of $[Fe(CN)_6]^{-3/-4}$ redox couple. Fig. 2 A–C show the Nyquist plots (Fig. 2A), impedance module plots (Fig. 2B) and the phase angles (ϕ) (Fig. 2C) vs. frequency for the bare GC, GC/SPE, GC/CRGO and CG/SPE/CRGO electrodes.

Fig. 2D shows the equivalent circuits, which best fitted the experimental data for the different electrodes. For bare GC electrodes, the Nyquist plot shows a semi-circle at high frequencies, due to the kinetic control of the electron transfer of the redox couple, while at low frequencies a straight line is found, corresponding to the diffusion control of the redox couple (Fig. 2A, symbol □) [43]. The contribution of the constant phase element was evidenced for the bare GC electrode in the frequency range from 100 to 4000 Hz (Fig. 2B and C, symbol □). The Randles equivalent circuit (Fig. 2D a) was the best fitted the experimental data for the bare GC electrode, whereR_s is the solution resistance, R_{ET} is the electron transfer resistance, CPE_{dl} is the constant phase element of the electrical double layer, and W is the Warburg element. From the fitting, the following values were obtained for the bare GC electrode: $R_s = 120\,\Omega$, $R_{ET} = 112\,\Omega$, $CPE_{dl} = 1.1 \times 10^{-5}\,F\,s^{-0.08}$ and $W = 406\,\Omega\,s^{-1/2}$.

The Nyquist plot for the GC/SPE modified electrode also shows a semi-circle at high frequencies, and a straight line at low frequencies (Fig. 2A, symbol ∇). The best fitting was obtained when the equivalent circuit showed in Fig. 2D b was used, where the constant phase element, CPE_c, refers to the presence of the enzyme, which acts as a dielectric, making difficult the electron transferof $[Fe(CN)_6]^{-3/-4}$ redox couple. Fig. 2B and C (symbol ∇) show that the contribution of the CPE is found in the same frequency range than for the bare GC electrode. From the fitting, the following values were found: $R_s = 66\,\Omega$, $R_{ET} = 1266\,\Omega$, $CPE_{dl} = 3.2 \times 10^{-6}\,F\,s^{-0.12}$, $CPE_c = 3.4 \times 10^{-4}\,F\,s^{-0.15}$ and $W = 627\,\Omega\,s^{-1/2}$.

The equivalent circuit that best fitted the experimental data for the GC/CRGO modified electrode was also that shown in Fig. 2D b. Casero et al. [44] previously used this same equivalent circuit to fit the impedance data for GC/GO electrodes. The CPE_c element corresponds to the impedance to the electron transfer generated by the hydroxyl, carbonyl and carboxyl groups that are in the basal plane of the CRGO and that are not affected by the chemical reduction process, since this treatment causes only the reduction of the epoxy groups [31]. Fig. 2A (symbol Δ) shows the Nyquist plot obtained for the GC/CRGO modified electrode, which shows only a straight line. The contribution of CPE in this modified electrode is observed at lower frequencies than for the bare GC electrode, i.e., in the frequency range from 0.1 to 100 Hz. The following values were obtained for the different elements of the equivalent circuit: $R_s = 100\,\Omega$, $R_{ET} = 62\,\Omega$, $CPE_{dl} = 3.5 \times 10^{-6}\,F\,s^{-0.15}$, $CPE_c = 7.9 \times 10^{-6}\,F\,s^{-0.13}$ and $W = 406\,\Omega\,s^{-1/2}$. For comparisons, Fig. S4 (Supporting Information) shows the Nyquist plot obtained for the GC/GO modified electrode. The following values were obtained for the different elements of the equivalent circuit described by Fig. 2D.b: $R_s = 100\,\Omega$, $R_{ET} = 670\,\Omega$, $CPE_{dl} = 3.95 \times 10^{-6}\,F\,s^{-0.15}$, $CPE_c = 3.36 \times 10^{-4}\,F\,s^{-0.13}$ and $W = 406\,\Omega\,s^{-1/2}$. These results also clearly show the lower resistance to charge transfer of CRGO than GO.

The Nyquist plot for the GC/SPE/CRGO modified electrode also shows a semi-circle and a linear line at high and low frequencies, respectively (Fig. 2A, symbol o). The equivalent circuit for this modified electrode (Fig. 2D c) is similar to that of the bare GC electrode, with the difference that it has an additional part, consisting of a resistance and a constant phase element in series, R_{Enz} and CPE_c, respectively. This new contribution to the total impedance would be caused by the enzyme/electrode electron transfer, which is not observed for the GC/SPE electrode. The contribution of CPE in this modified electrode is practically in the same frequency range than that of the bare GC electrode (Fig, 2C, symbol o). Values of the different elements of the equivalent circuit, obtained from the best fitting, were: $R_s = 118\,\Omega$, $R_{ET} = 4124\,\Omega$, $R_{Enz} = 5.3 \times 10^{-10}\,\Omega$, $CPE_{dl} = 1.1 \times 10^{-5}\,F\,s^{-0.18}$, $CPE_c = 6.3 \times 10^{-7}\,F\,s^{-0.12}$ and $W = 539\,\Omega\,s^{-1/2}$.

From the previous results, it is possible to infer that the CRGO decreases the resistance to the electron transfer, which would facilitate the direct electron transfer between the active site of the enzyme and the electrode surface. Fig. 2E shows the schemes corresponding to the different stages in the construction of the biosensor.

On the other hand, the EIS measurements were also carried out in 0.1 M PBS, pH 7.0 for the GG/SPE/CRGO electrode, in the absence of $[Fe(CN)_6]^{-3/-4}$ redox couple, in order to study only the enzyme/electrode interaction (see below). Fig. 3A shows the Nyquist plot obtained under these experimental conditions and Fig. 3B the corresponding Bode plots. The equivalent circuit used to perform the fitting is shown in Fig. 3C. It has a new element, C_a, which is the capacitance of surface processes [36].

From the results of the fitting, it is possible to determine the direct electron transfer rate constant, $k_{ET,2}$, which corresponds to Cp II/SPE redox couple [36], defined by Eq. (3).

$$k_{ET,2} = \frac{1}{2R_{ET}C_a} \quad (3)$$

As shown in Fig. 3A, it is not possible to observe the complete semi-circle in the Nyquist plot.The impossibility of performing measurements at frequencies in the order of μHz with our equipments does not allow that the full semicircle can be observed. The value of $k_{ET,2}$ estimated was $0.04\,s^{-1}$, in very good agreement with the value previously obtained by CV.

3.2.3. Amperometry

Fig. 4A shows the steady-state reduction currents (I_{ss}) obtained after the addition of different H_2O_2 aliquots. I_{ss} are obtained at 4 min for H_2O_2 concentrations ($c_{H_2O_2}$) lower than 2 μM, while they are obtained at 20 s for $c_{H_2O_2} \geq 2$ μM. Thus, the current is controlled by the transport of H_2O_2 from the solution bulk to the electrode surface at low concentrations of H_2O_2, while at high concentrations of H_2O_2 the limiting-step is the reaction rate because the H_2O_2 concentration on the electrode surface is equal to that of the solution bulk [17].

Fig. 4B shows the corresponding calibration curve. The linear section of the calibration curve is shown in the inset of Fig. 4B, which satisfies the Linearity Test, i.e., $F_{Experimental} < F_{Theoretical}$ [45]. Its sensitivity is $(4.4 \pm 0.4) \times 10^{-3}\,A\,M^{-1}$. Each point of the calibration curve is the average of six replicated measurements obtained using different modified electrodes. The linear concentration range was from 1.5×10^{-7} to 3.0×10^{-6} M. The LOD was 5.0×10^{-8} M.

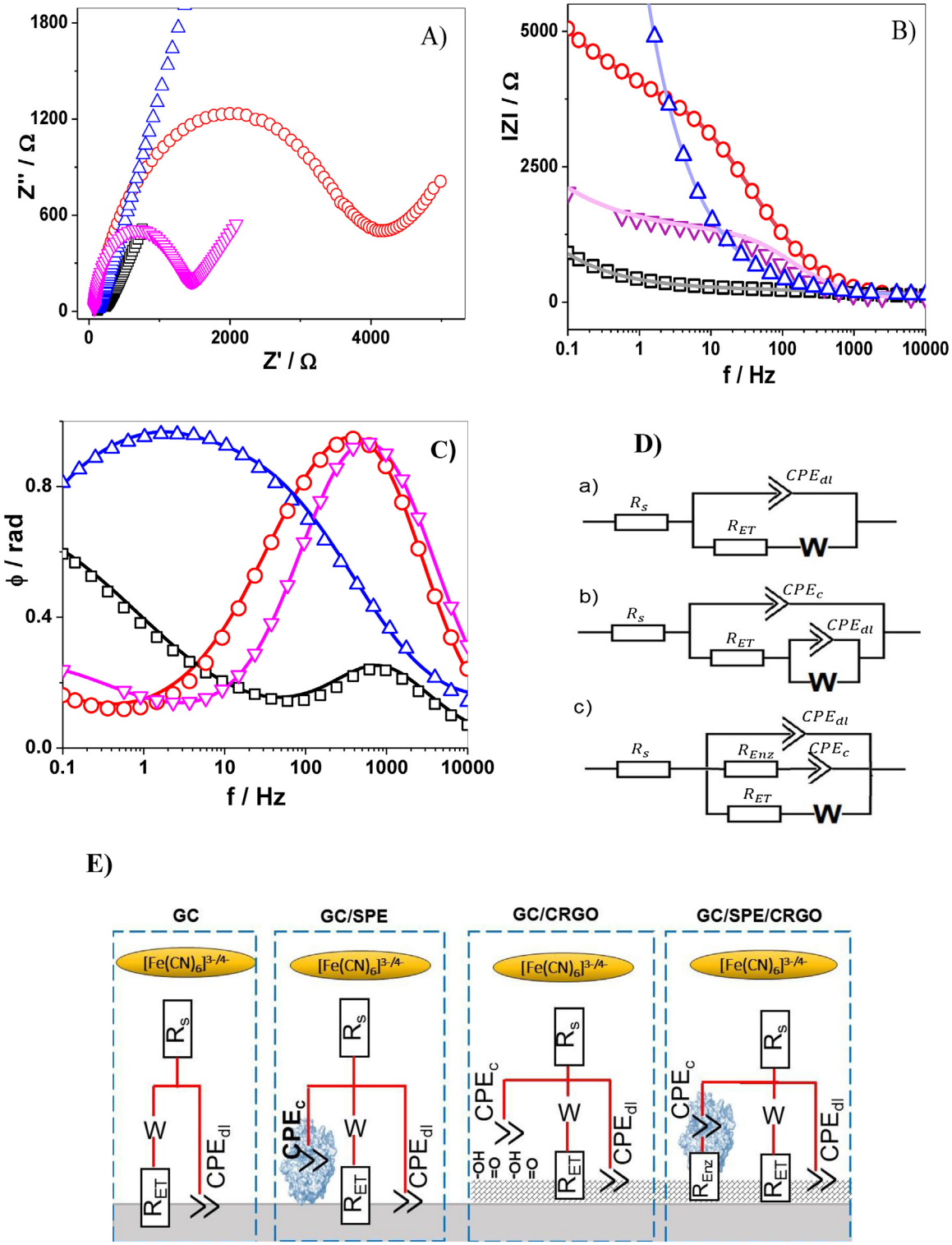

Fig. 2. Nyquist (A), impedance module (B), and phase angles (C) vs. frequency plots for the GC (□), GC/CRGO (Δ), GC/EPS/CRGO (O) and GC/SPE (∇) electrodesrecorded in 5×10^{-3} M $[Fe(CN)_6]^{-4/-3}$ + 0.1 M KCl aqueous solutions. The solid lines are the simulated impedance spectra. (D) Equivalent circuits which best fitted the experimental data for the different electrodes, i.e., for the bare GC (a), the GC/CRGO and GC/SPE (b) and GC/SPE/CRGO (c) electrodes. (E) Schemes for the equivalent circuits used. is the bare GC electrode, is the CRGO and is the SPE.

It was calculated following the modern IUPAC recommendations [45,46].

This LOD is much lower than those determined by other biosensors based on SPE (Table 1). The LOQ was 1.5×10^{-7} M (calculated as three times the LOD). At H_2O_2 concentrations greater than 48 μM, the current reaches the steady state, showing a typical Michaelis-Menten behavior.

It is well known that the chemical reactions involved in the catalytic cycle of peroxidases are irreversible. This causes that there is no upper limit on the reaction rate, not complying with the behavior predicted by Michaelis-Menten [49]. However, there is evidence that if only one of the three reactions involved is considered, the behavior of Michaelis-Menten can be observed [50].

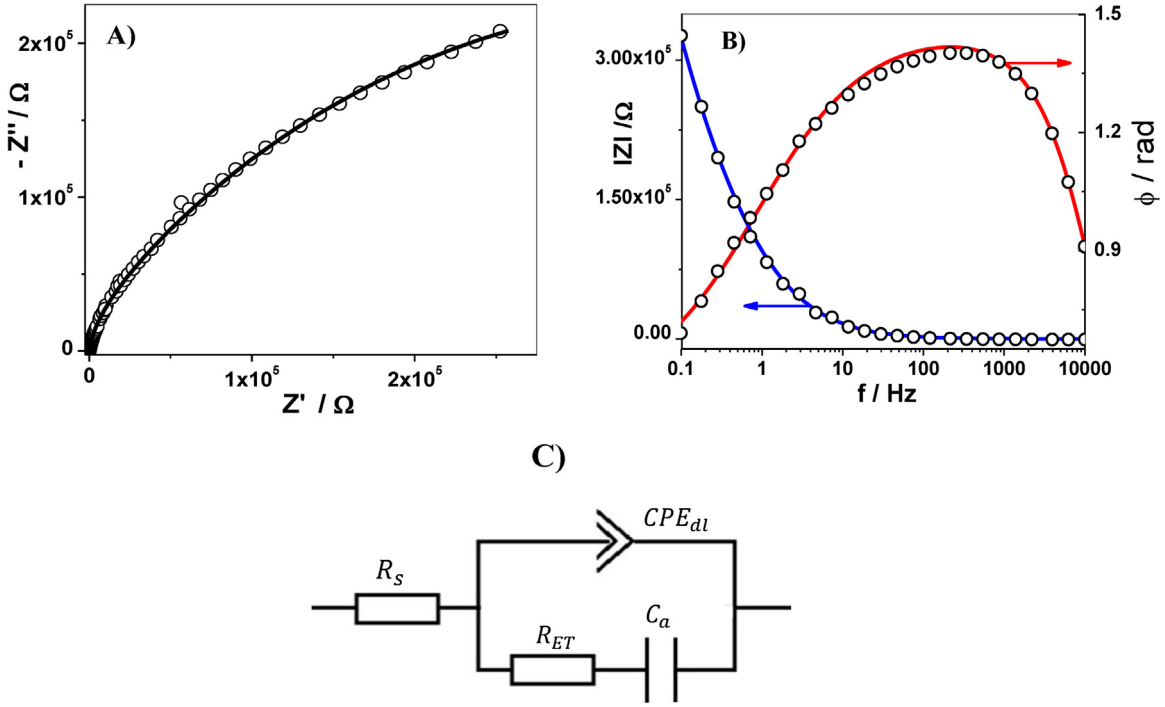

Fig. 3. Nyquist (A) and Bode (B) plots for the GC/SPE/CRGO electrode recorded in 0.1 M PBSpH 7.0. The arrows indicate the corresponding axes. (C) The equivalent circuit, which best fitted the experimental data.

Table 1
Characteristic parameters of different biosensors based on SPE.

Electrode	LOD/M	Linear range/M	Sensitivity/A M^{-1}	K_M^{app}/M	Reference
GC/SWCNHs/SPE	5×10^{-7}	$(0.02–1.2) \times 10^{-3}$	0.0166	4.88×10^{-3}	[15]
Sol–Gel Thin-Film Immobilized SPE[a]	5×10^{-7}	$(0.02–2.6) \times 10^{-3}$	0.0275	5.12×10^{-3}	[47]
GC/PVA-g-PVP/SPE[b]	1×10^{-7}	$(0.01–6.2) \times 10^{-3}$	0.0052	12.8×10^{-3}	[48]
GC/SPE/CRGO	5×10^{-8}	$(0.15–3) \times 10^{-6}$	0.0040	1.6×10^{-6}	This work

PVA-g-PVP: self-gelatinizable grafting copolymer of polyvinyl alcohol with 4-vinylpyridine.
[a] using methylene blue as redox mediator.
[b] using ferricyanide as redox mediator.

The Michaelis-Menten apparent constant (K_M^{app}) can be determined through both the Lineweaver-Burk and Eadie-Hofstee equations (ecs. 4 and 5, respectively) [41,49]:

$$\frac{1}{I_{ss}} = \frac{1}{I_{max}} + \frac{K_M^{app}}{I_{max}} \frac{1}{c_{H_2O_2}} \quad (4)$$

$$I_{ss} = -K_M^{app} \frac{I_{ss}}{c_{H_2O_2}} + I_{max} \quad (5)$$

where I_{max} is the current obtained at the maximum reaction rate, under saturation conditions. Values of $K_M^{app} = (1.6 \pm 0.4) \times 10^{-6}$ M and $I_{max} = (3.9 \pm 0.7) \times 10^{-8}$ A, and $K_M^{app} = (1.4 \pm 0.6) \times 10^{-6}$ M and $I_{max} = (4 \pm 1) \times 10^{-8}$ A were obtained for this biosensor using Eqs. (4) and (5), respectively.Values obtained by both methods are very similar. Both methods give the same results for small errors. However, when the error increases, both methods present differences, i.e., the Lineweaver-Burk method has better accuracy, and the Eadie-Hofstee method has better precision [51]. These K_M^{app} values are much lower than those determined for other biosensors based on SPE (Table 1), showing that the enzyme present in the SPE/CRGO composite has higher affinity toward H_2O_2 than other biosensors. Another important advantage of the proposed biosensor is that the use of a redox mediator is not necessary. Based on these results, the only advantages of other biosensors based on SPE described in the literature compared to the biosensor proposed in this paper is that they have a greater linear range and greater sensitivity [15,47,48] (Table 1). In addition, none of them were applied to the determination of H_2O_2 in real samples.The presence of interferences was only studied in those biosensors based on GC/SWCNHs/SPE [15], and sol-gel thin-film immobilized SPE [47].

On the other hand, amperograms recorded with the GC/SPE/CRGO electrode modified by different aliquots of H_2O_2 after performing a potential sweep from −0.5 to −1.7 V showed no change in current responses (results not shown). This behavior clearly shows that a sweep to very cathodic potentials causes the loss of the catalytic activity of the enzyme.

3.2.3.1. Statistical parameters of the biosensor. Reproducibility was studied by preparing four different modified electrodes. From the corresponding calibration curves a percentage variation coefficient (VC%) of 9% was obtained. Repeatability was determined by measuring the slopes of four calibration curves obtained with the same electrode. A VC% of 4% was calculated. The biosensor was stable during five days stored at 4 °C. Although these results show that the long-term stability of the biosensor is not optimal, it is important to note that its preparation is very simple and the LOD is very low. The rather low stability of the biosensor could be explained considering that the interaction between the SPE/CRGO composite and the GC electrode surface is given by physical adsorption.In addition, the rather low stability of the biosensor could be explained con-

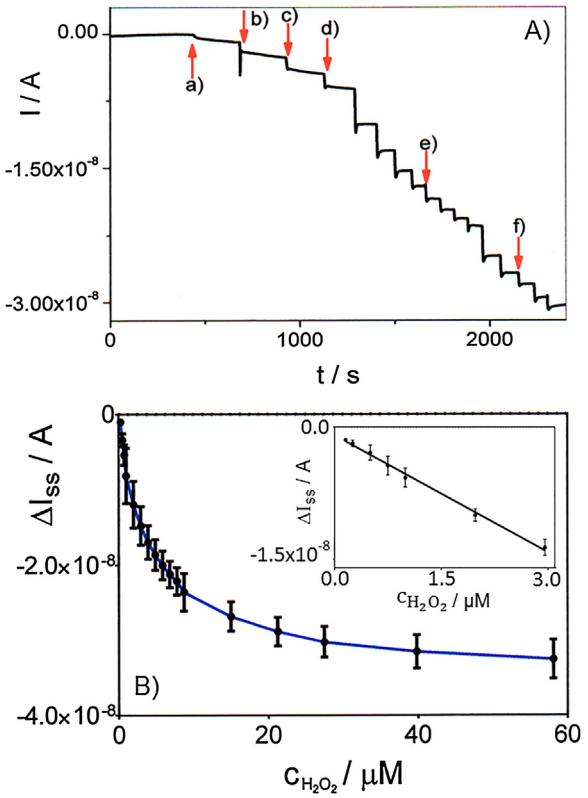

Fig. 4. (A) Plot of I vs. t for different aliquots of H_2O_2. (B) ΔI_{ss} vs. $c_{H_2O_2}$ plot.$c_{H_2O_2}$ = (a) 0.25, (b) 0.50, (c) 0.75, (d) 1.00, (e) 6.00 and (f) 20.00 μM. Inset of Fig. 4B shows the linear section of the calibration curve, which can be expressed by the linear least squares procedure as: $\Delta I_{SS} = (-4.4 \pm 0.4) \times 10^{-3} \times c_{H_2O_2}$ (M) − (7.9 ± 0.5) × 10^{-10} (A), linear correlation coefficient, r = 0.9989.

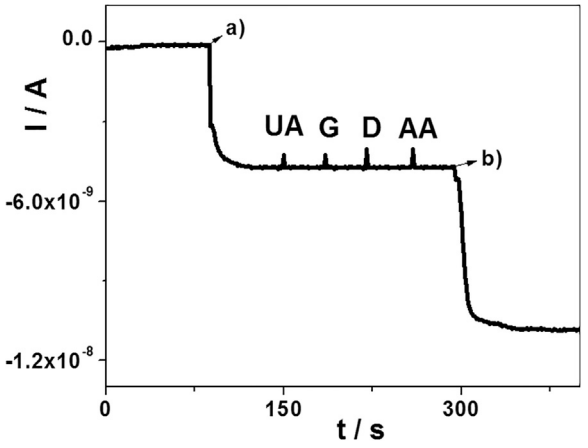

Fig. 5. Responses of the biosensor to the addition of aliquots of 1 μM H_2O_2 before (a) and after (b) the addition of uric acid (UA), glucose (G), dopamine (D) and ascorbic acid (AA) at a concentration of 100 μM.

sidering electrostatic repulsions between molecules of enzymes negatively charged at pH 7.0 because the isoelectric point of SPE is 3.9. However, the SPE/CRGO composite is stable during three months.

The selectivity of the biosensor towards the determination of H_2O_2 was evaluated by adding substances that are common interferences such as uric acid, glucose, dopamine and ascorbic acid [7,11,41]. Thus, the selectivity was studied using a solution 1 μM H_2O_2, to which each interferencewas added at a concentration of 100 μM. The addition of the aforementioned interferences did not produce any change in the current response (Fig. 5), showing that

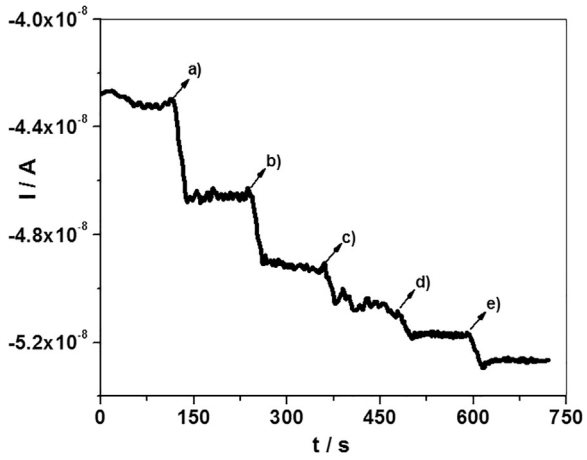

Fig. 6. Responses of the biosensor to the addition of a given aliquot of the commercial contact lens care solution (a) and different aliquots (b-e) of the H_2O_2solution. $c_{H_2O_2}$ = 0.25; 0.50; 0.75 and 1.00 μM from (b) to (e), respectively.

Table 2
Determination of H_2O_2 in contact lens care solutions. Each value is the average of three replicated measurements.

Samples	$c_{H_2O_2}$/μM	$c_{H_2O_2}$/μM[a]	Recovery/%
1	1	1.1 ± 0.1	110
2	1.5	1.4 ± 0.1	93
3	2	1.9 ± 0.2	95

[a] $c_{H_2O_2}$ calculated using the standard addition method.

they do not interfere in the determination of H_2O_2. These results show that the proposed biosensor is highly selective to determine H_2O_2.

3.2.3.2. Determination of H_2O_2 in a real sample. A 1:10 dilution of the commercial contact lens care solution was performed in PBS of pH 7.0.Then, a new 1: 2000 dilution was performed. After stabilizing the biosensor in the pH 7.0 PBS, an aliquot of the last diluted solution was injected into the electrochemical cell at a final volume of 2 mL. Then, different aliquots of the H_2O_2 commercial solution were added every two minutes. Fig. 6 shows the ammperograms obtained after these additions. Table 2 shows the concentrations of the prepared solutions and those calculated using the standard additions method, with the corresponding recovery percentages.

Under our experimental conditions, we have found that a better reproducibility in the determination of real samples is obtained when dilutions were performed. The GC/SPE/CRGO biosensor was also used for the determination of the sterigmatocystin mycotoxin in contaminated maize samples with very good results, which will give rise to a future scientific publication.

4. Conclusions

It was shown that the presence of chemical reduced graphene oxide in the soybean peroxidase enzyme/chemical reduced grapheme oxide composite used to modify the glassy carbon electrodes allows the direct electron transfer between the enzyme and the electrode surface. Thus, we developed a biosensor to determine H_2O_2 without the need to use any redox mediator. The biosensor shows a high affinity toward H_2O_2, a low limit of detection anda high selectivity. In addition, the biosensor is easy and quick to construct. UV–vis spectroscopy and scanning electron microscopy were used to demonstrate the chemical reduction of the graphene oxide. Electrochemical impedance spectroscopy was used to characterize the different stages in the process of the electrode surface

modification. The biosensor was applied to the determination of H_2O_2 in contact lens care solutions with a good accuracy and recovery percentages.

Acknowledgements

Financial supports from Agencia Nacional de Promoción Científica y Tecnológica (FONCYT) (PICT 2266/2014), Consejo Nacional de Investigaciones Científicas y Técnicas (CONICET) (PIP 112-201101-00184), Ministerio de Ciencia y Tecnología de la Provincia de Córdoba (MINCyT) (PID 050/2010), and Secretaría de Ciencia y Técnica (SECyT) (PPI 2016-2018, Res. 331/16) from Universidad Nacional de Río Cuarto are gratefully acknowledged. The authors thank to Dr. Gabriel Planes for his help in taking the SEM images. C. H. Díaz Nieto and J. C. López thank to CONICET for doctoral fellowships.

Appendix A. Supplementary data

Supplementary data associated with this article can be found, in the online version, at https://doi.org/10.1016/j.snb.2018.02.094.

References

[1] Y. Li, Biological properties of peroxide-containing tooth whiteners, Food Chem. Toxicol. 34 (1996) 887–904.
[2] EPA Chemicals under the TSCA (Toxic Substances Control Act). http://www.epa.gov/chemical-data-reporting.
[3] J. Ueda, N. Saito, Y. Shimazu, T. Ozawa, A comparison of scavenging abilities of antioxidants against hydroxyl radicals, Arch. Biochem. Biophys. 333 (1996) 377–384.
[4] N. Nasirizadeh, Z. Shekari, A. Nazari, M. Tabatabaee, Fabrication of a novel electrochemical sensor for determination of hydrogen peroxide in different fruit juice samples, J. Food Drug Anal. 24 (2016) 72–82.
[5] X.B. Kang, G.C. Pang, X.Y. Liang, M. Wang, J. Liu, W.M. Zhu, Study on a hydrogen peroxide biosensor based on horseradish peroxidase/GNPs-thionine/chitosan, Electrochim. Acta 62 (2012) 327–334.
[6] B. Rismetov, T.A. Ivandini, E. Saepudin, Y. Einaga, Electrochemical detection of hydrogen peroxide at platinum-modified diamond electrodes for an application in melamine strip tests, Diam. Relat. Mater. 48 (2014) 88–95.
[7] M.B. Gholivand, M. Khodadadian, Amperometric cholesterol biosensor based on the direct electrochemistry of cholesterol oxidase and catalase on a graphene/ionic liquid-modified glassy carbon electrode, Biosens. Bioelectron. 53 (2014) 472–478.
[8] J.K.A. Kamal, D.V. Behere, Thermal and conformational stability of seed coat soybean peroxidase, Biochemistry 41 (2002) 9034–9042.
[9] J.K.A. Kamal, D.V. Behere, Activity, stability and conformational flexibility of seed coat soybean peroxidase, J. Inorg. Biochem. 94 (2003) 236–242.
[10] Q. Lu, X. Chen, Y. Wu, S. Hu, Studies on direct electron transfer and biocatalytic properties of heme proteins in lecithin film, Biophys. Chem. 117 (2005) 55–63.
[11] Y. Zhang, J. Zhang, H. Wu, S. Guo, J. Zhang, Glass carbon electrode modified with horseradish peroxidase immobilized on partially reduced graphene oxide for detecting phenolic compounds, J. Electroanal. Chem. 681 (2012) 49–55.
[12] T. Gu, J. Wang, H. Xia, S. Wang, X. Yu, Direct electrochemistry and electrocatalysis of horseradish peroxidase immobilized in a DNA/chitosan-Fe_3O_4 magnetic nanoparticle bio-complex film, Materials 7 (2014) 1069–1083.
[13] L. Shi, X. Liu, W. Niu, H. Li, S. Han, J. Chen, G. Xu, Hydrogen peroxide biosensor based on direct electrochemistry of soybean peroxidase immobilized on single-walled carbon nanohorn modified electrode, Biosens. Bioelectron. 24 (2009) 1159–1163.
[14] B.J. Ryan, N. Carolan, C. O'Fagain, Horseradish and soybean peroxidases: comparable tools for alternative niches? Trends Biotechnol. 24 (2006) 355–363.
[15] A. Henriksen, O. Mirza, C. Indiani, K. Teilum, G. Smulevich, K.G. Welinder, M. Gajhede, Structure of soybean seed coat peroxidase: a plant peroxidase with unusual stability and haem-apoprotein interactions, Protein Sci. 10 (2001) 108–115.
[16] P.M. Guto, C.V. Kumar, J.F. Rusling, Thermostable peroxidase-polylysine films for biocatalysis at 90 °C, J. Phys. Chem. B 111 (2007) 9125–9131.
[17] T. Ruzgas, L. Gorton, J. Emnéus, G. Marko-Varga, Kinetic models of horseradish peroxidase action on a graphite electrode, J. Electroanal. Chem. 391 (1995) 41–49.
[18] J.E. Frew, H.A.O. Hill, Direct and indirect electron transfer between electrodes and redox proteins, Eur. J. Biochem. 172 (1988) 261–269.
[19] R.A. Marcus, N. Sutin, Electron transfers in chemistry and biology, Biochim. Biophys. Acta 811 (1985) 265–322.
[20] A. Martín, A. Escarpa, Graphene The cutting–edge interaction between chemistry and electrochemistry, Trends Anal. Chem. 56 (2014) 13–26.
[21] D.A.C. Brownson, D.K. Kampouris, C.E. Banks, Graphene electrochemistry: fundamental concepts through to prominent applications, Chem. Soc. Rev. 41 (2012) 6944–6976.
[22] S. Pei, H.-M. Cheng, The reduction of graphene oxide, Carbon 50 (2012) 3210–3228.
[23] D. Krishnan, F. Kim, J. Luo, R. Cruz-Silva, L.J. Cote, H.D. Jang, J. Huang, Energetic graphene oxide: challenges and opportunities, Nano Today 7 (2012) 137–152.
[24] P. Tjissen, Enzymes for Immunoassays, in: R.H. Burdon, P.H. Van Knippenberg (Eds.), Practice and Theory of Enzyme Immunoassays, Elsevier Amsterdam, New York, Oxford, 1985, pp. 173–220.
[25] A.D. Hildebrandt, I. Roots, Reduced nicotinamide adenine dinucleotide phosphate (NADPH)-dependent formation and breakdown of hydrogen peroxide during mixed function oxidation reactions in liver microsomes, Arch. Biochem. Biophys. 171 (1975) 385–397.
[26] A.S. Bondarenko, G.A. Ragoisha, in: A.L. Pomerantsev (Ed.), Progress in Chemometrics Research, Nova Science Publishers, New York, USA, 2005, pp. 89–102 (the program is available in: www.abc.chemistry.bsu.by/vi/analyser/).
[27] D.C. Marcano, D.V. Kosynkin, J.M. Berlin, A. Sinitskii, Z. Sun, A. Slesarev, L.B. Alemany, W. Lu, J.M. Tour, Improved synthesis of graphene oxide, ACS Nano 4 (2010) 4806–4814.
[28] Y. Guo, S. Guo, J. Ren, Y. Zhai, S. Dong, E. Wang, Cyclodextrin functionalized graphene nanosheets with high supramolecular recognition capability: synthesis and host-guest inclusion for enhanced electrochemical performance, ACS Nano 4 (2010) 4001–4010.
[29] D. Montgomery, G. Runger, Probabilidad y Estadística, 2nd ed., Mc Graw Hill. Interamericana Editores, México, 2000.
[30] S.D. Brown, R. Tauler, B. Walczak (Eds.), Comprehensive Chemometrics, Chemical and Biochemical Data Analysis, Elsevier, London, UK, 2009.
[31] Z.-S. Wu, W. Ren, L. Gao, J. Zhao, Z. Chen, B. Liu, D. Tang, B. Yu, C. Jiang, H.-M. Cheng, Synthesis of graphene sheets with high electrical conductivity and good thermal stability by hydrogen arc discharge exfoliation, ACS Nano 3 (2009) 411–417.
[32] L. Gorton, A. Lindgren, T. Larsson, F.D. Munteanu, T. Ruzgas, I. Gazaryan, Direct electron transfer between heme-containing enzymes and electrodes as basis for third generation biosensors, Anal. Chim. Acta 400 (1999) 91–108.
[33] Z. Brusova, E. Magner, Kinetics of oxidation of hydrogen peroxide at hemin-modified electrodes in nonaqueous solvents, Bioelectrochemistry 76 (2009) 63–69.
[34] E. Torres, M. Ayala, Biocatalysis Based on Heme Peroxidases. Peroxidases as Potential Industrial Biocatalysts, Springer, Germany, 2010.
[35] E. Csöregi, G. Jönsson-Pettersson, L. Gorton, Mediator less electrocatalytic reduction of hydrogen peroxide at graphite electrodes chemically modified with peroxidases, J. Biotechnol. 30 (1993) 315–337.
[36] J. Li, S.Dong, The electrochemical study of oxidation-reduction properties of horseradish peroxidase, J. Electroanal. Chem. 431 (1997) 19–22.
[37] A.J. Bard, L.R. Faulkner, Electrochemical Methods. Fundamentals and Applications, 2nd ed., J. Wiley & Sons, Inc, New York, USA, 2001.
[38] R.S. Freire, C.A. Pessoa, L.D. Mello, L.T. Kubota, Direct electron transfer: an approach for electrochemical biosensors with higher selectivity and sensitivity, J. Braz. Chem. Soc. 14 (2003) 230–243.
[39] E. Laviron, General expression of the linear potential sweep voltammogram in the case of diffusionless electrochemical systems, J. Electroanal. Chem. 101 (1979) 19–28.
[40] W. Sun, F. Hou, S. Gong, L. Han, W. Wang, F. Shi, J. Xi, X. Wang, G. Li, Direct electrochemistry and electrocatalysis of hemoglobin on three-dimensional graphene modified carbon ionic liquid electrode, Sens. Actuators B Chem. 219 (2015) 331–337.
[41] Y.-L. Zhang, C.-X. Zhang, H.-X. Shen, Studies on electrocatalytically kinetic behavior of horseradish peroxidase at salt bridge supported bilayer lipid membrane, Anal. Lett. 33 (2000) 2425–2439.
[42] M. Fazilati, A biosensor by using modified glassy carbon electrode with HRP enzyme and ZrO_2 nanoparticles for detect of H_2O_2, Ann. Biol. Res. 3 (2012) 5350–5357.
[43] E. Barsoukov, J.R. Mac Donald, Impedance Spectroscopy: Theory, Experiment, and Applications, 2nd ed., J. Wiley, New Jersey, USA, 2005.
[44] E. Casero, A.M. Parra-Alfambra, M.D. Petit-Domínguez, F. Pariente, E. Lorenzo, C. Alonso, Differentiation between graphene oxide and reduced graphene by electrochemical impedance spectroscopy (EIS), Electrochem. Commun. 20 (2012) 63–66.
[45] H.C. Goicoechea, A.C. Olivieri, La Calibración en Química Analítica, 1st ed., Ediciones UNL, Argentina, 2007.
[46] A.C. Olivieri, Practical guidelines for reporting results in single- and multi-component analytical calibration: a tutorial, Anal. Chim. Acta 868 (2015) 10–22.
[47] B.Q. Wang, B. Li, Z.X. Wang, G.B. Xu, Q. Wang, S.J. Dong, Sol–Gel thin-gilm immobilized soybean peroxidase biosensor for the amperometric determination of hydrogen peroxide in acid medium, Anal. Chem. 71 (1999) 1935–1939.
[48] B. Wang, B. Li, G. Cheng, S. Dong, Acid-stable amperometric soybean peroxidase biosensor based on a self-gelatinizable grafting copolymer of polyvinyl alcohol and 4-vinylpyridine, Electroanal 7 (2001) 555–558.
[49] H.B. Dunford, Heme Peroxidases, J. Wiley Inc. Sons Inc., New York USA, 1999.
[50] J.N. Rodríguez-López, M.A. Gilabert, J. Tudela, R.N.F. Thorneley, F. García-Cánovas, Reactivity of horseradish peroxidase compound II toward substrates: kinetic evidence for a two-step mechanism, Biochemistry 39 (2000) 13201–13209.

[51] F. Ranaldi, P. Vanni, E. Giachetti, What students must know about the determination of enzyme kinetic parameters, Biochem. Educ. 27 (1999) 87–91.

Biographies

César H. Díaz Nieto obtained his graduate in Chemistry (2012) from Salta National University (Salta, Argentina) and his Ph. D. in Chemistry (2017) from Rio Cuarto National University (Rio Cuarto, Argentina) in the group of Electroanalysis at the Chemistry Department, Faculty of Exact, Physico-Chemical and Natural Sciences (Río Cuarto National University). At present, he has a post-doctoral fellowship from Argentine Research Council (CONICET) in the Research and Development of Advanced Materials and Energy Storage Centre from Jujuy (CIDMEJu) (Jujuy, Argentina). He was an active member of the Electroanalysis Group at the Chemistry Department, and his research interests was focused on the development of electroanalytical techniques for the determination of sterigmatocystin mycotoxin as well as the design and characterization of chemical sensors, and electrochemical biosensors based on nano-structured materials.

Adrian M. Granero obtained his Ph.D. in Chemistry (2009) from Río Cuarto National University (UNRC, Río Cuarto, Argentina). He carried out a Postdoctoral training (2009–2012) at Río Cuarto National University, and at Córdoba National University (UNC, Córdoba, Argentina). Currently, he is Researcher at Argentine Research Council (CONICET). His research interest focus on several subjects, such as electrochemistry of mycotoxins, natural antioxidants, and the design of sensors/biosensors for the determination of these substances in real matrixes. Actually, he has over fifteen peer reviewed papers, five book chapters and one book.

Jimena C. López obtained her graduate in Chemistry (2013) from Río Cuarto National University (Río Cuarto, Argentina) and she is doing her Ph. D. in Chemistry at Rio Cuarto National University in the group of Electroanalysis at the Chemistry Department, Faculty of Exact, Physico-Chemical and Natural Sciences (Río Cuarto National University). At present, she has a doctoral fellowship from Argentine Research Council (CONICET). She is an active member of the Electroanalysis Group at the Chemistry Department, and her research interests is focused on the electrochemical behavior of natural antioxidants as well as the development and characterization of chemical sensors, and electrochemical biosensors based on nano-structured materials.

Gastón D. Pierini obtained his Ph. D in Chemistry (2015) from National University of the South (Bahía Blanca, Argentina). He is now doing a Fellowship from Argentine Research Council (CONICET) at Río Cuarto National University (UNRC, Río Cuarto, Argentina). His research now is focusing in the development of electrochemical methods to quality control in food samples.

Gustavo J. Levin obtained his Ph.D. in Biochemistry – Biotechnology area (2009) at the University of Buenos Aires (UBA, CABA, Argentina). He completed postdoctoral training at the University of Buenos Aires (2009–2011) and at the University Complutense of Madrid (UCM, Madrid, Spain) (2013–2014). He is currently Researcher at the Argentine Research Council (CONICET, Argentina). His research focuses on various to subjects such as purification of enzymes from agro industrial wastes, enzymes of thermophilic microorganisms, biocatalysts and their potential industrial applications. It has more than thirteen peer-reviewed papers, and one book chapter.

Héctor Fernández obtained his Ph. D. in Chemistry (1978) from Río Cuarto National University (UNRC) (Río Cuarto, Argentina). He did the postdoctoral training (1980–1982) at the University of New York at Buffalo, Buffalo (USA). Currently, he is Full Professor at the UNRC and Principal Researcher at Argentine Research Council (CONICET). He was Dean of the Faculty of Exact, Physico-Chemical and Natural Sciences (UNRC, 1992–1999) and Head of the Department of Chemistry at the Faculty of Exact, Physico-Chemical and Natural Sciences (2001–2004). He was President of the Argentinean Society of Analytical Chemists (2007–2009). His research interest focuses on several subjects, such as electrochemistry of mycotoxins, hormones and synthetic and natural antioxidants, studies on ultramicroelectrodes and electrodes modified by self-assembled monolayers of thiols, carbon nanotubes, antibodies, etc., and their use for electroanalytical applications. Development of electroanalytical techniques for the determination of antioxidants, mycotoxins and hormones in real matrixes (plants, cereal, foods, sera of animal origin, etc., respectively). Design and characterization of chemical sensors, electrochemical (bio)sensors and immune-electrodes based on nanostructured materials. He has over eightysix peer-reviewed papers, and eight book chapters. He is co-author of a book and he has been the editor of a book. Prof. Fernández has been a member of the Editorial Board of J. Biosensors and Bioelectronics, and actually is editor of The Polish Journal of Environmental Studies. He is an AAQA, AAIFQ and SIBAE fellow.

María A. Zon obtained her Ph. D. in Chemistry (1985) from Río Cuarto National University (Río Cuarto, Argentina). She did the postdoctoral training at the Cordoba University (Córdoba, España) between 1990 and 1992. She is Full Professor at the Río Cuarto National University and Principal Researcher at the Argentine Research Council (CONICET). She has been the secretary of the Argentinean Society of Analytical Chemists (2007–2009). Her research interest focuses on the development of electrochemical (bio) sensors by using nano-materials for the determination of different substrates such as mycotoxins, synthetic and natural antioxidants, and hormones. She has over 75 peer-reviewed papers, eight book chapters and she is co-author of a book. She has been co-editor of an electroanalytical book. Prof. Zon is an AAQA,AAIFQ and SIBAE fellow.